Coupling the vortex dynamics with collective excitations in Bose-Einstein Condensate due modulation of the scattering length

R. P. Teles, V. S. Bagnato and F. E. A. dos Santos

Instituto de Física de São Carlos, USP, Caixa Postal 369,

13560-970 São Carlos, São Paulo, Brazil

Abstract

Here we analyze the collective excitations as well as the expansion of a trapped Bose-Einstein condensate with a vortex line at its center. To this end, we propose a variational method where the variational parameters have to be carefully chosen in order to produce reliable results. Our variational calculations agree with numerical simulations of the Gross-Pitaevskii equation. The system considered here turns out to exhibit four collective modes of which only three can be observed at a time depending of the trap anisotropy. We also demonstrate that these collective modes can be excited using well **established** experimental methods such as modulation of the s-wave scattering length.

I. INTRODUCTION

In this work, we are interested in the dynamics of a trapped Bose-Einstein condensate (BEC) containing a line vortex at its center. Here we are particularly interested in obtaining the collective oscillation modes of the system which couples the vortex core oscillations with the oscillations of the condensate external dimensions. The interest in this problem is motivated by the fact that these oscillations can be measured in the laboratory by moving the atomic cloud out of its equilibrium configuration by using the Feshbach resonance in order to modulate the scattering length [1–5]. These oscillations are also studied in other physical systems such as two-species condensates [6], BCS-BEC crossover [7–9], and superfluid Helium [10]. From the theoretical point of view, we are **interested in** how the size of the vortex core oscillates with respect to the external dimensions of the cloud. The mode with the smallest oscillation frequency is the quadrupole mode which occurs when the longitudinal and radial sizes of condensate oscillate out phase. The breathing mode requires more energy to be excited since the change in the density of the atomic cloud imposes a greater resistance against deviation from its equilibrium configuration than in the case of quadrupole excitations [11, 12].

The frequency shifts of quadrupole oscillations due presence of a singly charged vortex have already been explored analytically for positive scattering lengths using a sum rule approach [13], as well as, the effects of lower dimensional geometry on this frequency spitting of quadrupole oscillations [14].

In Refs. [15–17], the dynamics of normal modes for a single vortex has been studied using hydrodynamic models, which focus on the vortex motion with respect to the center-of-mass of the condensate. This concept was also used in the case of multicomponent Bose-Einstein condensates [18]**, and to describe the shape and behavior of a single perturbed along the vortex line [19].**

Preliminary calculations using a variational calculation with a Gaussian Ansatz, which does not take into account the independent variation of the vortex core size [3, 6, 18, 20], shows a small shift in the frequencies of the aforementioned modes (Figure 1). This shift has already been obtained via a hydrodynamic approximation in Refs. [12] and [21]. Thus we can expect the frequency of the monopole (breathing) mode to decrease while the quadrupole frequency increases in the presence of the vortex.

To calculate the dynamics of a vortex with charge ℓ in a more consistent way with the physical reality, which allows for the coupling between vortex core and the external dimensions

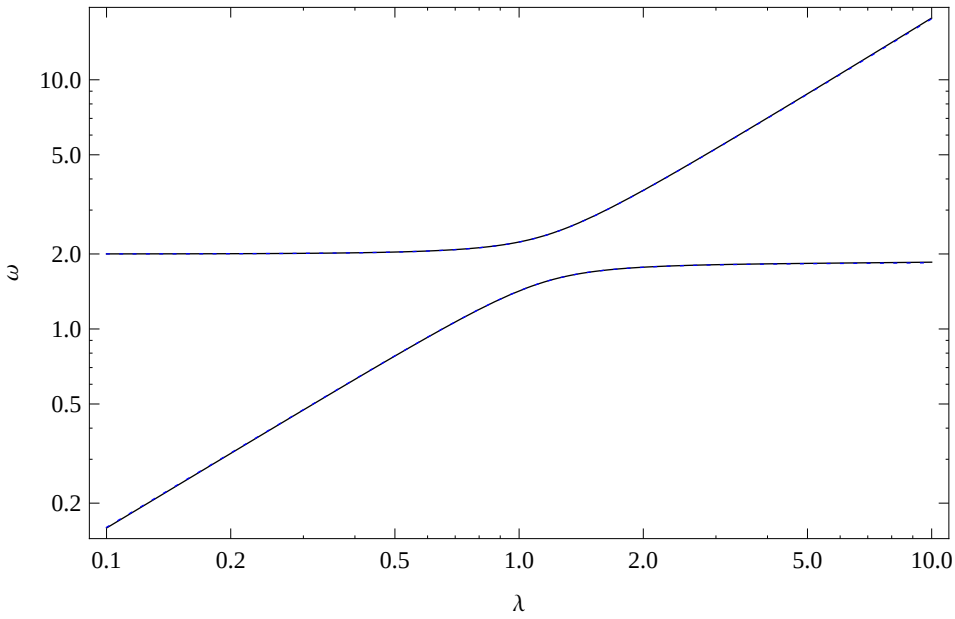

Figure 1: (Color online) Oscillation frequencies from Gaussian Ansatz without taking into account the independent variation of the vortex core size. Upper lines correspond the frequencies of the breathing mode as a function of the harmonic trap anisotropy, whereas lower lines represent the frequencies of the quadrupole mode. Solid (black) lines correspond to a vortex-free Gaussian-profile while dotted (blue) lines describe a profile with a singly charged vortex. Note that ϖ is normalized by the frequency of the radial direction ω_ρ.

of condensate, we could naïvely use a Thomas-Fermi (TF) Ansatz [22]

$$\psi\left(\rho,\varphi,z,t\right)=A\left(t\right)\left[\frac{\rho^{2}}{\rho^{2}+\xi\left(t\right)^{2}}\right]^{\frac{\ell}{2}}\sqrt{1-\frac{\rho^{2}}{R_{\rho}\left(t\right)^{2}}-\frac{z^{2}}{R_{z}\left(t\right)^{2}}}\exp\left[i\ell\varphi+iB_{\rho}\left(t\right)\frac{\rho^{2}}{2}+iB_{z}\left(t\right)\frac{z^{2}}{2}\right], \tag{1}$$

where $R_\rho(t)$ and $R_z(t)$ are the condensate sizes in radial ($\hat{\rho}$) and axial ($\hat{z}$) directions, $\xi(t)$ is the size of vortex core, $B_\rho(t)$ and $B_z(t)$ represent the components of the velocity field, and then we calculate the equations of motion for the five variational parameters (ξ, R_ρ, R_z, B_ρ, B_z). Following these calculations, the equations of motion would be linearized. For the Ansatz (1), this procedure leads to imaginary frequencies which are not consistent with the stable configuration where a singly charged ($\ell = 1$) vortex resides at the center of the condensate. The linearized equations of motion can be written in a matrix form according to

$$M\ddot{\delta}+V\delta=0, \tag{2}$$

where δ is the vector with components given by deviations of the variational parameters from their equilibrium values. The solution of (2) is a linear combination of oscillatory modes whose

oscillation frequencies obey the equation

$$\prod_n \varpi_n^2 = \det\left(M^{-1}V\right) = \frac{\det V}{\det M}. \tag{3}$$

In order to ensure that all frequencies ϖ_n are real, we must have $\det V/\det M > 0$. We know that $\det V > 0$ since its sign reflects the sign of the variational parameters which represents the external dimensions of the cloud in the stationary situation. Therefore $\det M$ must also be positive. In the case of Ansatz (1) with $\ell = 1$, such conditions are not satisfied since $\det M < 0$, which indicates that there is something wrong with Ansatz (1). In previous works [17, 18, 23, 24], since the authors did not consider the size of the vortex core as a variational parameter, this problem did not appear. Indeed, the problem relies on the fact that the phase of the **wave function has to be** modified.

In Section II, the necessary requirements for the wave function phase are discussed in order to give support to our variational method. Section III has the calculation based on the new Ansatz and the corresponding equations of motion are obtained. The collective modes considering the coupling between vortex and atomic cloud are obtained via linearization of the equations of motion, thus resulting in new collective oscillations (section IV). In section V, we showed that such excitation modes can be excited using the scattering length modulation. The free expansion was also calculated in order to complement a previous work [24]. Finally, section VII contains the conclusions on our subject of study.

II. WAVE-FUNCTION PHASE

We start with the Lagrangian density,

$$\mathcal{L} = \frac{i\hbar}{2}\left(\psi^*\frac{\partial\psi}{\partial t} - \psi\frac{\partial\psi^*}{\partial t}\right) - \frac{\hbar^2}{2m}\left|\nabla\psi\right|^2 - V\left(\mathbf{r}\right)\left|\psi\right|^2 - \frac{g}{2}\left|\psi\right|^4, \tag{4}$$

whose extremization leads to the Gross-Pitaevskii equation (GPE):

$$i\hbar\frac{\partial\psi}{\partial t} = \left[-\frac{\hbar^2}{2m}\nabla^2 + V\left(\mathbf{r}\right) + g\left|\psi\right|^2\right]\psi, \tag{5}$$

where $V\left(\mathbf{r}\right) = \frac{1}{2}m\omega_\rho^2\left(\rho^2 + \lambda^2 z^2\right)$ is an external potential, the trap anisotropy is $\lambda = \omega_z/\omega_\rho$, and g is the coupling constant. The complex field $\psi\left(\mathbf{r},t\right)$ can be written as an amplitude profile multiplied by a respective phase, as follows:

$$\psi\left(\mathbf{r},t\right) = f\left(w_l,\mathbf{r}\right)e^{iS(\chi_l,\mathbf{r})}, \tag{6}$$

where

$$S\left(\chi_l, \mathbf{r}\right) = \ell\varphi + \sum_l \chi_l \phi_l(\mathbf{r}). \tag{7}$$

We denoted both, $w_l = w_l\left(t\right)$ and $\chi_l = \chi_l\left(t\right)$, respectively, as the amplitude and phase variational parameters. In principle, $\{\phi_l\left(\mathbf{r}\right)\}$ should be a complete set of functions but in our present approximation, we use only a representative incomplete set of functions. Substituting (6) and (7) into (4), the Lagrangian $L = \int \mathcal{L} d^3\mathbf{r}$ becomes

$$L = -\hbar \sum_l \dot{\chi}_l \int d^3\mathbf{r} f^2 \phi_l - \frac{\hbar^2}{2m} \sum_l \chi_l^2 \int d^3\mathbf{r} f^2 \left|\nabla \phi_l\right|^2 - \int d^3\mathbf{r} \left(\frac{\hbar^2}{2m} \left|\nabla f\right|^2 + V f^2 + \frac{g}{2} f^4 \right). \tag{8}$$

In order to account for the dynamics of all three variational parameters **(R_ρ, R_z, and ξ)** in f we include a variational phase which also contains three variational parameters. This way we chose the following trial function:

$$S(\rho, \varphi, z, t) = \ell\varphi + B_\rho(t)\frac{\rho^2}{2} + C(t)\frac{\rho^4}{4} + B_z(t)\frac{z^2}{2}. \tag{9}$$

Now the velocities field is

$$\vec{v}\left(\rho, \varphi, z, t\right) = \frac{\hbar}{m}\left[B_\rho\left(t\right)\rho + C\left(t\right)\rho^3\right]\hat{\rho} + \frac{\hbar\ell}{m}\hat{\varphi} + \frac{\hbar}{m} B_z\left(t\right) z\hat{z}, \tag{10}$$

which includes the movement of the vortex size ξ in opposite direction to the radius $R_\rho$when B_ρ and C have opposite signs. As the superfluid current is connected to the density variation, it is desirable that both, amplitude and phase, have the same number of variational parameters. The Ansatz (9) also leads to linearized equations of motion (2) with $\det M > 0$ which is consistent with the stability of the condensate with a singly charged vortex at its center.

III. EQUATIONS OF MOTION

Now we correct the Thomas-Fermi Ansatz according to the discussion in section II. This leads to the following trial function:

$$\begin{aligned}\psi\left(\mathbf{r}, t\right) =& \sqrt{\frac{N}{R_\rho(t)^2 R_z(t) A_0\left[\xi\left(t\right)/R_\rho\left(t\right)\right]}} \left[\frac{\rho^2}{\rho^2 + \xi\left(t\right)^2}\right]^{\frac{\ell}{2}} \sqrt{1 - \frac{\rho^2}{R_\rho\left(t\right)^2} - \frac{z^2}{R_z\left(t\right)^2}} \\ & \times \exp\left[i\ell\varphi + iB_\rho\left(t\right)\frac{\rho^2}{2} + iC(t)\frac{\rho^4}{4} + iB_z\left(t\right)\frac{z^2}{2}\right],\end{aligned} \tag{11}$$

with

$$A_0(\alpha) = \frac{2\pi^{3/2}(\ell)!}{15\alpha^{2\ell}\left(\frac{3}{2}+\ell\right)!}\left[\left(3+2\ell\alpha^2\right){}_2F_1\left(\ell,1+\ell;\frac{5}{2}+\ell;-\frac{1}{\alpha^2}\right)\right.$$
$$\left.-2\ell\left(1+\alpha^2\right){}_2F_1\left(1+\ell,1+\ell;\frac{5}{2}+\ell;-\frac{1}{\alpha^2}\right)\right], \tag{12}$$

where, for simplicity we define $\alpha(t) = \xi(t)/R_\rho(t)$, ${}_pF_q(a_1,\ldots,a_p;b_1,\ldots,b_q;x)$ are the hypergeometric functions, $\xi(t)$ is the size of the vortex core, $R_\rho(t)$ is the condensate size in radial direction ($\hat{\rho}$), and $R_z(t)$ is the condensate size in axial direction ($\hat{z}$). The wave function (11) has integration domain defined by $1-\frac{\rho^2}{R_\rho^2}-\frac{z^2}{R_z^2}\geq 0$, where the wave function is approximately an inverted parabola (TF-shape), except for the central vortex. The trapping potential shape sets the condensate dimensions. To organize our calculations, we split the Lagrangian so that it is a sum $L = L_{time} + L_{kin} + L_{pot} + L_{int}$ of the following terms:

$$L_{time} = \frac{i\hbar}{2}\int d^3\mathbf{r}\left[\psi^*(\mathbf{r},t)\frac{\partial\psi(\mathbf{r},t)}{\partial t} - \psi(\mathbf{r},t)\frac{\partial\psi^*(\mathbf{r},t)}{\partial t}\right]$$
$$= -\frac{N\hbar}{2}\left(D_1\dot{B}_\rho R_\rho^2 + D_2\dot{B}_z R_z^2 + \frac{1}{2}D_3\dot{C}R_\rho^4\right), \tag{13}$$

$$L_{kin} = -\frac{\hbar^2}{2m}\int d^3\mathbf{r}\left[\nabla\psi^*(\mathbf{r},t)\right]\left[\nabla\psi(\mathbf{r},t)\right]$$
$$= -\frac{N\hbar^2}{2m}\left[D_1B_\rho^2R_\rho^2 + D_2B_z^2R_z^2 + 2D_3B_\rho C R_\rho^4 + \ell^2R_\rho^{-2}(D_4+D_5) + D_6C^2R_\rho^6\right], \tag{14}$$

$$L_{pot} = -\frac{1}{2}m\omega_\rho^2\int d^3\mathbf{r}\left(\rho^2+\lambda^2z^2\right)\psi^*(\mathbf{r},t)\,\psi(\mathbf{r},t)$$
$$= -\frac{N}{2}m\omega_\rho^2\left(D_1R_\rho^2 + \lambda^2D_2R_z^2\right), \tag{15}$$

$$L_{int} = -\frac{g}{2}\int d^3\mathbf{r}\left[\psi^*(\mathbf{r},t)\,\psi(\mathbf{r},t)\right]^2$$
$$= -\frac{N^2gD_7}{2R_\rho^2R_z}, \tag{16}$$

with the functions $D_i(\alpha)$ given by

$$D_1(\alpha) = A_0(\alpha)^{-1} \frac{2\pi^{3/2}(1+\ell)!}{21\alpha^{2\ell}\left(\frac{5}{2}+\ell\right)!}\left[\left(3+2\ell\alpha^2\right){}_2F_1\left(\ell,2+\ell;\frac{7}{2}+\ell;-\frac{1}{\alpha^2}\right)\right.$$
$$\left.-2\ell\left(1+\alpha^2\right){}_2F_1\left(1+\ell,2+\ell;\frac{7}{2}+\ell;-\frac{1}{\alpha^2}\right)\right], \tag{17}$$

$$D_2(\alpha) = A_0(\alpha)^{-1} \frac{\pi^{3/2}(\ell)!}{4\alpha^{2\ell}\left(\frac{7}{2}+\ell\right)!}\left[(7+2\ell){}_2F_1\left(\ell,1+\ell;\frac{7}{2}+\ell;-\frac{1}{\alpha^2}\right)\right.$$
$$\left.-(5+2\ell){}_3F_2\left(\ell,1+\ell,\frac{7}{2}+\ell;\frac{5}{2}+\ell,\frac{9}{2}+\ell;-\frac{1}{\alpha^2}\right)\right], \tag{18}$$

$$D_3(\alpha) = A_0(\alpha)^{-1} \frac{2\pi^{3/2}(2+\ell)!}{27\alpha^{2\ell}\left(\frac{7}{2}+\ell\right)!}\left[(3+2\ell){}_2F_1\left(\ell,3+\ell;\frac{9}{2}+\ell;-\frac{1}{\alpha^2}\right)\right.$$
$$\left.-2\ell\left(1+\alpha^2\right){}_2F_1\left(1+\ell,3+\ell;\frac{9}{2}+\ell;-\frac{1}{\alpha^2}\right)\right], \tag{19}$$

$$D_4(\alpha) = A_0(\alpha)^{-1} \frac{2\pi^{3/2}(\ell-1)!}{3\alpha^{2\ell}\left(\frac{1}{2}+\ell\right)!}\left[\left(1-2\ell\alpha^2\right){}_2F_1\left(\ell,2+\ell;\frac{3}{2}+\ell;-\frac{1}{\alpha^2}\right)\right.$$
$$\left.+2\ell\left(1+\alpha^2\right){}_2F_1\left(1+\ell,2+\ell;\frac{3}{2}+\ell;-\frac{1}{\alpha^2}\right)\right], \tag{20}$$

$$D_5(\alpha) = A_0(\alpha)^{-1} \frac{2\pi^{3/2}(\ell-1)!}{9\alpha^{2\ell}\left(\frac{1}{2}+\ell\right)!}\left[\left(3+2\ell\alpha^2\right){}_2F_1\left(\ell,\ell;\frac{3}{2}+\ell;-\alpha^2\right)\right.$$
$$\left.-2\ell\left(1+\alpha^2\right){}_2F_1\left(\ell,1+\ell;\frac{3}{2}+\ell;-\frac{1}{\alpha^2}\right)\right], \tag{21}$$

$$D_6(\alpha) = A_0(\alpha)^{-1} \frac{2\pi^{3/2}(3+\ell)!}{33\alpha^{2\ell}\left(\frac{9}{2}+\ell\right)!}\left[\left(3+2\ell\alpha^2\right){}_2F_1\left(\ell,4+\ell;\frac{11}{2}+\ell;-\frac{1}{\alpha^2}\right)\right.$$
$$\left.-2\ell\left(1+\alpha^2\right){}_2F_1\left(1+\ell,4+\ell;\frac{11}{2}+\ell;-\frac{1}{\alpha^2}\right)\right], \tag{22}$$

$$D_7(\alpha) = A_0(\alpha)^{-2} \frac{2\pi^{3/2}(2\ell)!}{\alpha^{4\ell}\left(\frac{7}{2}+\ell\right)!}{}_2F_1\left(2\ell,1+2\ell;\frac{9}{2}+2\ell;-\frac{1}{\alpha^2}\right). \tag{23}$$

For simplicity we can scale the variational parameters of the Lagrangian as well as the time in order to make them dimensionless,

$$\begin{aligned}
R_\rho(t) &\to a_{osc} r_\rho(t),\\
R_z(t) &\to a_{osc} r_z(t),\\
\xi(t) &\to a_{osc} r_\xi(t),\\
B_\rho(t) &\to a_{osc}^{-2} \beta_\rho(t),\\
B_z(t) &\to a_{osc}^{-2} \beta_z(t),\\
C(t) &\to a_{osc}^{-4} \zeta(t),\\
t &\to \omega_\rho^{-1} \tau,
\end{aligned}$$

where the harmonic oscillator length is $a_{osc} = \sqrt{\hbar/m\omega_\rho}$ and the dimensionless interaction

parameter is $\gamma = Na_s/a_{osc}$. Thus the Lagrangian becomes

$$L = -\frac{N\hbar\omega_\rho}{2}\left[D_1 r_\rho^2\left(\dot{\beta}_\rho + \beta_\rho^2 + 1\right) + D_2 r_z^2\left(\dot{\beta}_z + \beta_z^2 + \lambda^2\right)\right.$$
$$\left. + D_3 r_\rho^4\left(\frac{1}{2}\dot{\zeta} + 2\beta_\rho\zeta\right) + \ell^2 r_\rho^{-2}\left(D_4 + D_5\right) + D_6\zeta^2 r_\rho^6 + D_7\frac{4\pi\gamma}{r_\rho^2 r_z}\right]. \tag{24}$$

The Euler-Lagrange equations

$$\frac{d}{dt}\left(\frac{\partial L}{\partial \dot{q}_i}\right) - \frac{\partial L}{\partial q_i} = 0, \tag{25}$$

for each one of the six variational parameters from Lagrangian (24) lead to the six differential equations:

$$\beta_\rho - \frac{\dot{r_\rho}}{r_\rho} - \frac{D_1'\dot{\alpha}}{2D_1} + \frac{D_3 r_\rho^2\zeta}{D_1} = 0, \tag{26}$$

$$\beta_z - \frac{\dot{r_z}}{r_z} - \frac{D_2'\dot{\alpha}}{2D_2} = 0, \tag{27}$$

$$\zeta - \frac{D_3\dot{r_\rho}}{D_6 r_\rho} - \frac{D_3\dot{\alpha}}{4D_6 r_\rho^2} + \frac{D_3\beta_\rho}{D_6 r_\rho^2} = 0, \tag{28}$$

$$D_1 r_\rho\left(\dot{\beta}_\rho + \beta_\rho^2 + 1\right) + D_3 r_\rho^3\left(\dot{\zeta} + 4\beta_\rho\zeta\right) -$$
$$\frac{\ell^2}{r_\rho^3}\left(D_4 + D_5\right) + 3D_6\zeta^2 r_\rho^5 - D_7\frac{4\pi\gamma}{r_\rho^3 r_z} = 0, \tag{29}$$

$$D_2 r_z\left(\dot{\beta}_z + \beta_z^2 + \lambda^2\right) - D_7\frac{2\pi\gamma}{r_\rho^2 r_z^2} = 0, \tag{30}$$

$$D_1' r_\rho^2\left(\dot{\beta}_\rho + \beta_\rho^2 + 1\right) + D_2' r_z^2\left(\dot{\beta}_z + \beta_z^2 + \lambda^2\right) + D_3' r_\rho^4\left(\frac{1}{2}\dot{\zeta} + 2\beta_\rho\zeta\right) +$$
$$\frac{\ell^2}{r_\rho^2}\left(D_4' + D_5'\right) + D_6'\zeta^2 r_\rho^6 - D_7'\frac{4\pi\gamma}{r_\rho^2 r_z} = 0. \tag{31}$$

Solving these equations for the parameters in the wave function phase, we have:

$$\beta_\rho = \frac{\dot{r_\rho}}{r_\rho} + F_1\dot{\alpha}, \tag{32}$$

$$\beta_z = \frac{\dot{r_z}}{r_z} + F_2\dot{\alpha}, \tag{33}$$

$$\zeta = F_3\frac{\dot{\alpha}}{r_\rho^2}, \tag{34}$$

where

$$F_1 = \frac{D_3' D_3 - 2D_1' D_6}{4\left(D_3^2 - D_1 D_6\right)}, \tag{35}$$

$$F_2 = \frac{D_2'}{2D_2}, \tag{36}$$

$$F_3 = \frac{2D_1' D_3 - D_1 D_3'}{4\left(D_3^2 - D_1 D_6\right)}. \tag{37}$$

Replacing (32), (33), and (34) into equations (29), (30), and (31), we reduce our six coupled equations to only three, which are given by:

$$D_1\left(\ddot{r_\rho}+r_\rho\right)+G_1 r_\rho\ddot{\alpha}+G_2 r_\rho\dot{\alpha}^2+G_3\dot{r_\rho}\dot{\alpha}-G_4\frac{\ell^2}{r_\rho^3}-D_7\frac{4\pi\gamma}{r_\rho^3 r_z}=0, \tag{38}$$

$$D_2\left(\ddot{r_z}+\lambda^2 r_z\right)+G_5 r_z\ddot{\alpha}+G_6 r_z\dot{\alpha}^2+G_7\dot{r_z}\dot{\alpha}-D_7\frac{2\pi\gamma}{r_\rho^2 r_z^2}=0, \tag{39}$$

$$\begin{aligned}D_1' r_\rho\left(\ddot{r_\rho}+r_\rho\right)+D_2' r_z\left(\ddot{r_z}+\lambda^2 r_z\right)+\left(G_8 r_\rho^2+G_9 r_z^2\right)\ddot{\alpha}+\left(G_{10} r_\rho^2+G_{11} r_z^2\right)\dot{\alpha}^2\\ +\left(G_{12} r_\rho\dot{r_\rho}+G_{13} r_z\dot{r_z}\right)\dot{\alpha}+G_{14}\frac{\ell^2}{r_\rho^2}+D_7'\frac{4\pi\gamma}{r_\rho^2 r_z}=0,\end{aligned} \tag{40}$$

with

$$G_1 = D_1F_1+D_3F_3, \tag{41}$$

$$G_2 = D_1\left(F_1^2+F_1'\right)+D_3\left(4F_1F_3+F_3'\right)+3D_6F_3^2, \tag{42}$$

$$G_3 = 2\left(D_1F_1+D_3F_3\right)=2G_1, \tag{43}$$

$$G_4 = D_4+D_5, \tag{44}$$

$$G_5 = D_2F_2, \tag{45}$$

$$G_6 = D_2\left(F_2^2+F_2'\right), \tag{46}$$

$$G_7 = 2D_2F_2=2G_5, \tag{47}$$

$$G_8 = D_1'F_1+\frac{1}{2}D_3'F_3, \tag{48}$$

$$G_9 = D_2'F_2, \tag{49}$$

$$G_{10} = D_1'\left(F_1^2+F_1'\right)+D_3'\left(\frac{1}{2}F_3'+2F_1F_3\right)+D_6'F_3^2, \tag{50}$$

$$G_{11} = D_2'\left(F_2^2+F_2'\right), \tag{51}$$

$$G_{12} = 2D_1'F_1+D_3'F_3, \tag{52}$$

$$G_{13} = 2D_2'F_2=2G_9, \tag{53}$$

$$G_{14} = D_4'+D_5'. \tag{54}$$

The terms $D_1 r_\rho$, $D_2\lambda^2 r_z$, $D_1' r_\rho^2$, and $D_2' r_z^2$ come from the trapping term L_{pot}, which can be neglected in the case of a freely expanding condensate. The parameter γ indicates the terms generated by the atomic interaction potential, while the fractions proportional to r_ρ^{-2} and r_ρ^{-3} come from the kinetic energy contribution due to the presence of the vortex with charge ℓ. The remaining factors represent the coupling between the outer dimensions of the condensate and the vortex core.

Making the velocities ($\dot{r_\rho}$, $\dot{r_z}$,$\dot{\alpha}$) and accelerations ($\ddot{r_\rho}$, $\ddot{r_z}$, $\ddot{\alpha}$) equal to zero leads to the

equations for the stationary solution:

$$D_1 r_{\rho 0} = G_4 \frac{\ell^2}{r_{\rho 0}^3} + D_7 \frac{4\pi\gamma}{r_{\rho 0}^3 r_{z0}}, \tag{55}$$

$$D_2 \lambda^2 r_{z0} = D_7 \frac{2\pi\gamma}{r_{\rho 0}^2 r_{z0}^2}, \tag{56}$$

$$D_1' r_{\rho 0}^2 + D_2' \lambda^2 r_{z0}^2 = -G_{14} \frac{\ell^2}{r_{\rho 0}^2} - D_7' \frac{4\pi\gamma}{r_{\rho 0}^2 r_{z0}}, \tag{57}$$

where r_ρ, r_z, and r_ξ take their respective equilibrium values $r_{\rho 0}$, r_{z0}, and $r_{\xi 0}$. We apply the Newton's method to solve the coupled stationary equations (55)–(57). The value of the atomic interaction parameter used from now on in this paper is $\gamma = 800$, which is close to the value used in Rubidium experiments [25].

IV. COLLECTIVE EXCITATIONS

For small deviations from the equilibrium configuration, we assume $r_\rho(t) \to r_{\rho 0} + \delta\rho(t)$, $r_z(t) \to r_{z0} + \delta z(t)$, $\alpha(t) \to \alpha_0 + \delta\alpha(t)$, and neglect all terms of order two or higher in (38)–(40). This leads to the linearized matrix equation

$$\begin{pmatrix} D_1 & 0 & G_1 r_{\rho 0} \\ 0 & D_2 & G_5 r_{z0} \\ D_1' r_{\rho 0} & D_2' r_{z0} & G_8 r_{\rho 0}^2 + G_9 r_{z0}^2 \end{pmatrix} \begin{pmatrix} \ddot{\delta\rho} \\ \ddot{\delta z} \\ \ddot{\delta\alpha} \end{pmatrix} +$$

$$\begin{pmatrix} D_1 + 3G_4 \frac{\ell^2}{r_{\rho 0}^4} + D_7 \frac{12\pi\gamma}{r_{\rho 0}^4 r_{z0}} & D_7 \frac{4\pi\gamma}{r_{\rho 0}^3 r_{z0}^2} & D_1' r_{\rho 0} - G_4' \frac{\ell^2}{r_{\rho 0}^3} - D_7' \frac{4\pi\gamma}{r_{\rho 0}^3 r_{z0}} \\ D_7 \frac{4\pi\gamma}{r_{\rho 0}^3 r_{z0}^2} & D_2 \lambda^2 + D_7 \frac{4\pi\gamma}{r_{\rho 0}^2 r_{z0}^3} & D_2' \lambda^2 r_{z0} - D_7' \frac{2\pi\gamma}{r_{\rho 0}^2 r_{z0}^2} \\ 2D_1' r_{\rho 0} - 2G_{14} \frac{\ell^2}{r_{\rho 0}^3} - D_7' \frac{8\pi\gamma}{r_{\rho 0}^3 r_{z0}} & 2D_2' \lambda^2 r_{z0} - D_7' \frac{4\pi\gamma}{r_{\rho 0}^2 r_{z0}^2} & D_1'' r_{\rho 0}^2 + D_2'' \lambda^2 r_{z0}^2 + G_{14}' \frac{\ell^2}{r_{\rho 0}^2} + D_7'' \frac{4\pi\gamma}{r_{\rho 0}^2 r_{z0}} \end{pmatrix} \begin{pmatrix} \delta\rho \\ \delta z \\ \delta\alpha \end{pmatrix}$$

$$= 0, \tag{58}$$

which defines the matrices M and V, appearing in Eq.(2). Solving the characteristic equation,

$$\det\left(M^{-1}V - \varpi^2 I\right) = 0, \tag{59}$$

results in the frequency of the collective modes of oscillation. Now the determinants $\det M$ and $\det V$ are both positive for $\ell = 1$. Meaning that we are in the lower energy state for the case of a central vortex in a Bose-Einstein condensate. Since (59) is a cubic equation of ϖ^2, we have three pair of frequencies $\pm\varpi_n$ $(n = z, \rho, \xi)$. There are three frequencies ϖ_n and four modes of oscillation in total, of which only three modes can be simultaneously observed depending on the anisotropy λ of harmonic potential as shown in fig.2. Among these four modes, two of them represent monopole oscillations while the other two represent quadrupole oscillations of

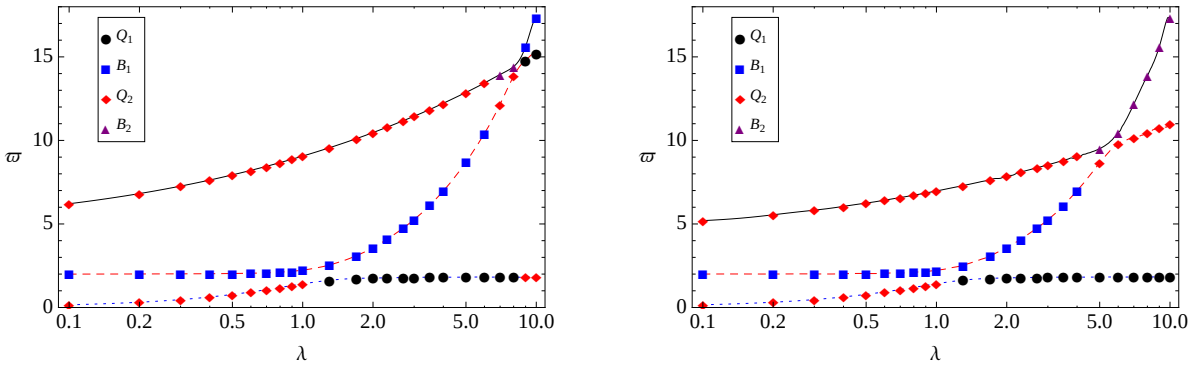

(a) $\ell = 1$ (b) $\ell = 2$

Figure 2: (Color online) Oscillation frequencies as a function of trap anisotropy in a condensate containing a singly (a) and doubly (b) charged vortex at its center. Solid (black) line is ϖ_ξ, dashed (red) line is ϖ_ρ, and dotted (blue) line is ϖ_z.

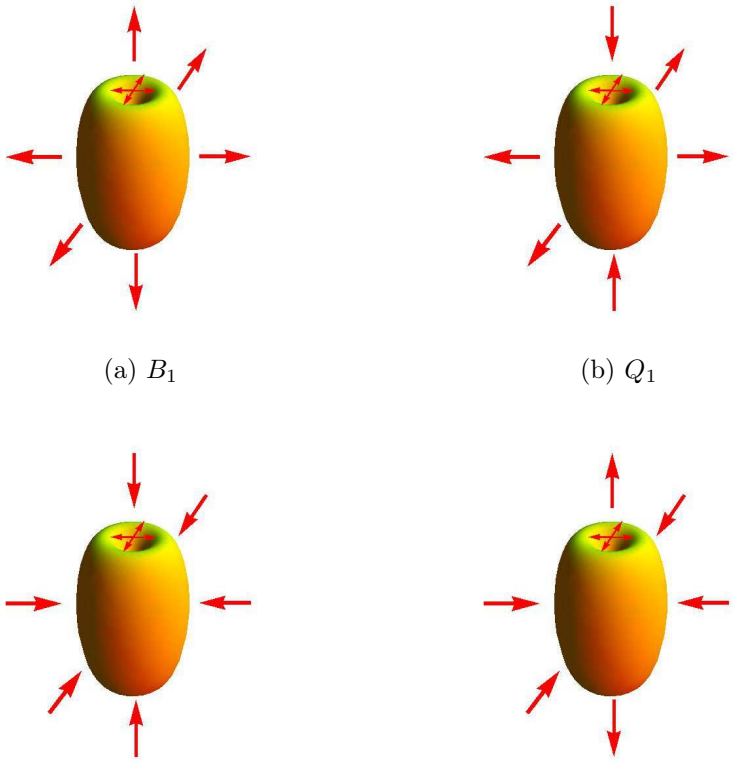

(a) B_1 (b) Q_1

(c) B_2 (d) Q_2

Figure 3: (Color online) Schematic representation of collective modes. B_1 mode has all components oscillating in phase. B_2 mode has r_ξ oscillating out of phase with r_ρ and r_z. Q_1 mode has r_z oscillation out of phase with r_ξ and r_ρ. Q_2 mode has r_ρ oscillation out of phase with r_ξ and r_z.

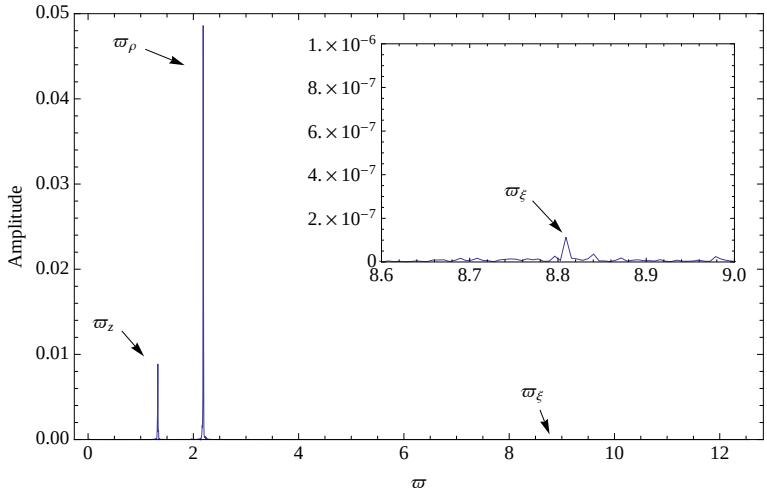

Figure 4: Excitation spectrum obtained from a numerical simulation of the GPE [26]. We set $\gamma = 800$, $\ell = 1$, $\tilde{\mu} = 20.74$, and $\lambda = 0.9$.ϖ_n are the frequencies of the oscillation modes from less energetic (ϖ_z) to more energetic (ϖ_ξ). The analytical values are $\varpi_z = 1.317$, $\varpi_\rho = 2.166$, and $\varpi_\xi = 8.874$.

the atomic cloud. The B_1 mode (fig.3a) is characterized by having all condensate components r_i $(i = z, \rho, \xi)$ oscillating in phase, however B_2 mode (fig.3c) presents r_ξ oscillating out of phase with r_ρ and r_z. The Q_1 mode (fig.3b) shows that r_z oscillation is out of phase with r_ξ and r_ρ, which are in phase with each other. However, in Q_2 mode (fig.3d) the oscillations of r_z and r_ξ are in phase with each other, being the r_ρ oscillation out of phase. Extrapolating to an ideal situation where $\gamma = 0$, the equations of motions (38)–(40) can be decoupled. This way, the ϖ_z (lower frequency) represents only a r_z oscillation, ϖ_ρ (middle frequency) represents only a r_ρ oscillation, and ϖ_ξ (upper frequency) represents only a r_ξ oscillation.

Numerical simulations where performed in order to validate our results (fig.4). Frequency values ϖ_n in the variational calculations differ from numerical values by less than 1%.

In fig.2a, for $0.1 \leq \lambda \leq 1$, exist two Q_2-like modes. The difference between them comes from the fact that vortex core oscillation amplitude which is two orders of magnitude lower at the less energetic mode. The same happens when $\ell = 2$ (fig.2b), i.e., the vortex core is almost still for the lower frequency in the same interval of λ.

The solid lines in fig.2 correspond to the mode with largest amplitude for the vortex-core oscillations. As can be seen, the excitation frequency ϖ_ξ of this mode lowers as the vortex circulation increases. It means that the energy necessary to excite it will be lower if ℓ is increased. However, we must point out that our results apply only for the cases where $r_\xi \ll r_\rho$.

V. SCATTERING LENGTH MODULATION

One of the mechanisms used for exciting collective modes is via modulation of the s-wave scattering length. This technique has been already applied to excite the lowest-lying quadrupole mode in a Lithium experiment [1]. Therefore, we consider the time-dependent scattering length:

$$a_s(t) = a_0 + \delta a \cos(\Omega t). \tag{60}$$

This is equivalent to make $\gamma \to \gamma(\tau)$, thus giving:

$$\gamma(\tau) = \gamma_0 + \delta\gamma \cos(\Omega\tau). \tag{61}$$

Where γ_0 is the average value of the interaction parameter $\gamma(\tau)$, $\delta\gamma$ is the modulation amplitude, and Ω is the excitation frequency. Substituting (61) into (58) and keeping only first-order terms ($\delta\rho$, δz, $\delta\alpha$, and $\delta\gamma$), we obtain a nonhomogeneous linear equation

$$M\ddot{\delta} + V\delta = P\cos(\Omega\tau) \tag{62}$$

with

$$P = 2\pi\delta\gamma \begin{pmatrix} \frac{2D_7}{r_{\rho 0}^3 r_{z0}} \\ \frac{D_7}{r_{\rho 0}^2 r_{z0}^2} \\ \frac{D_7'}{r_{\rho 0}^2 r_{z0}} \end{pmatrix}. \tag{63}$$

A particular solution of (62) is

$$\delta_\gamma(\tau) = \left(M^{-1}V - \Omega^2\right)^{-1} M^{-1} P\cos(\Omega\tau). \tag{64}$$

Projecting the vector $\delta_\gamma(\tau)$ in the base δ_n ($n = z, \rho, \xi$) of the eigenvectors of the homogenous equation associated to Eq.(62), we obtain

$$\langle\delta_n|\delta_\gamma(\tau)\rangle = \frac{\langle\delta_n|M^{-1}P\rangle}{\varpi_n^2 - \Omega^2}\cos(\Omega\tau). \tag{65}$$

Since **the scalar product $|\langle\delta_n|M^{-1}P\rangle|$ is always positive**, it shows that specific collective modes can be excited using a scattering length modulation with small amplitude $\delta\gamma$ and frequency Ω close to one of the resonance frequency ϖ_n. In fig.5, we see the results from a numerical solution of Eqs.(38)–(40) considering a time-dependent interaction $\gamma(\tau)$ according to Eq.(61). There we can see the beat behavior corresponding to a superposition of the frequencies $\Omega = 6$ and $\varpi_\xi = 6.13$.

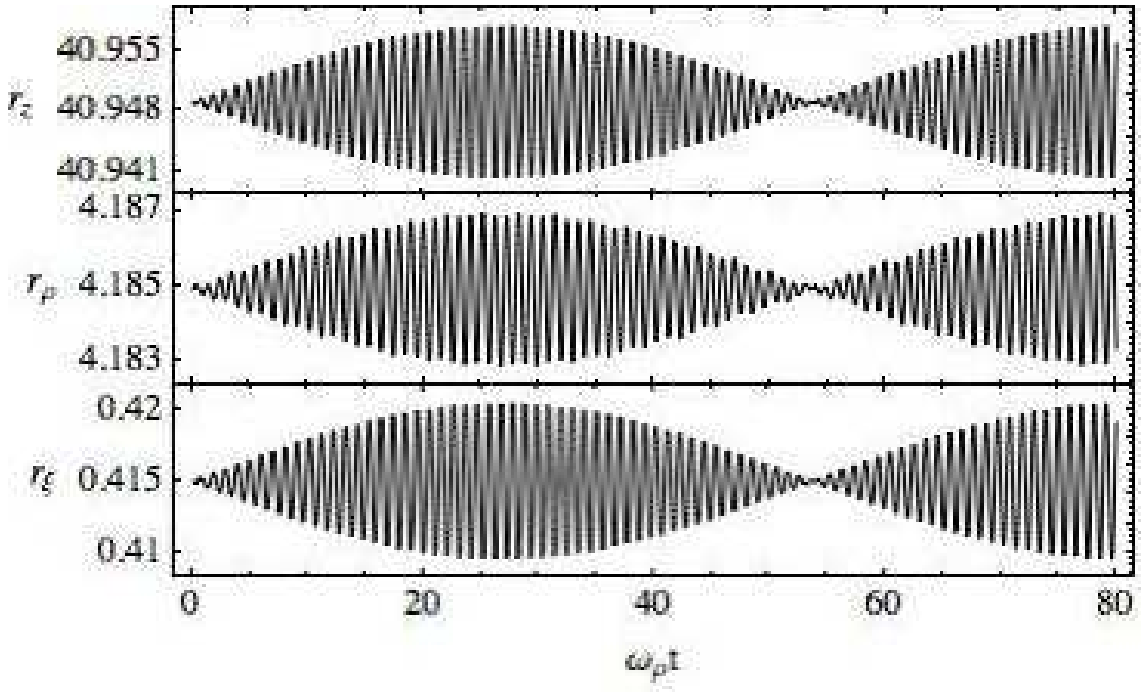

(a)

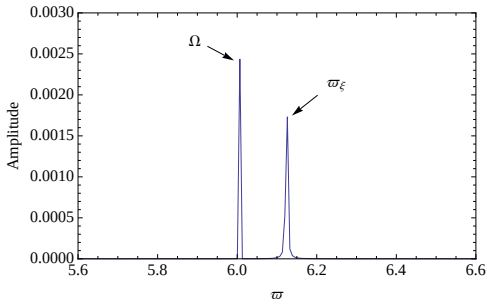

(b)

Figure 5: Numerical solution of Eqs.(38)–(40) with a time-dependent interaction $\gamma(\tau)$ **(a)**. **(b)** is the excitation spectrum obtained from variational calculation, where $\varpi_\xi \approx 6.13$ is close to the value calculated in Eq.(59). We excited the collective mode Q_2 ($\varpi_\xi = 6.21$) of a condensate with cigar shape ($\lambda = 0.1$, $\gamma_0 = 800$) via scattering modulation with amplitude $\delta\gamma = 0.4$ and frequency $\Omega = 6$.

VI. FREE EXPANSION

The time-of-flight pictures constitute the most common method to measure vortices in BEC. This method of switch off the magneto-optical trap and letting atomic cloud expand freely for some time, typically ten milliseconds and then taking a picture of the expanded cloud [5, 27–31]. For this purpose we use the equations of motion (38)–(40) without the terms arising from

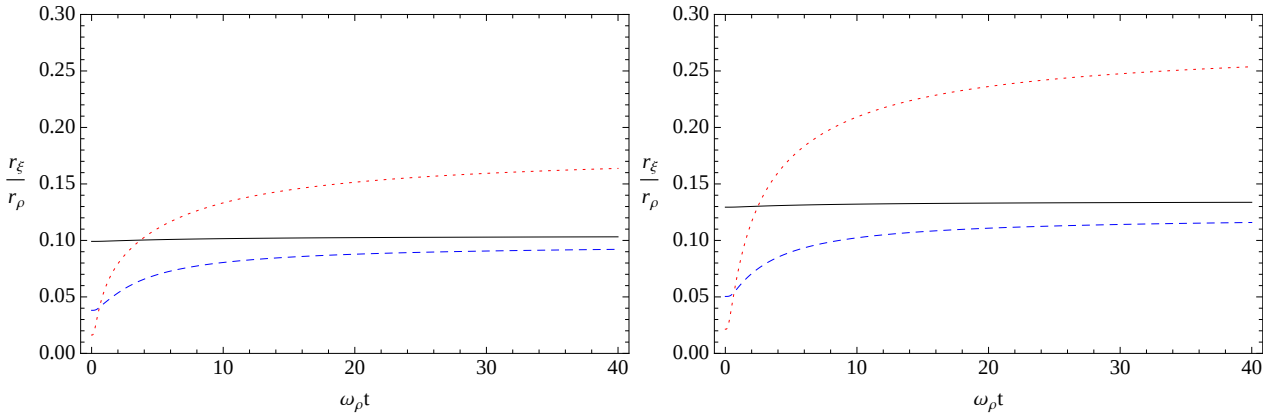

(a) $\ell = 1$ (b) $\ell = 2$

Figure 6: (Color online) Ratio between vortex core size and radial cloud size for different trap anisotropies while in free expansion. The solid (black) line corresponds to a prolate condensate ($\lambda = 0.1$), the dashed (blue) line to the isotropic case ($\lambda = 1$), and the dotted (red) line to a oblate condensate ($\lambda = 8$).

the harmonic potential, i.e.,

$$D_1\ddot{r_\rho} + G_1 r_\rho \ddot{\alpha} + G_2 r_\rho \dot{\alpha}^2 + G_3 \dot{r_\rho}\dot{\alpha} - G_4 \frac{\ell^2}{r_\rho^3} - \frac{4D_7\gamma}{r_\rho^3 r_z} = 0, \tag{66}$$

$$D_2\ddot{r_z} + G_5 r_z \ddot{\alpha} + G_6 r_z \dot{\alpha}^2 + G_7 \dot{r_z}\dot{\alpha} - \frac{2D_7\gamma}{r_\rho^2 r_z^2} = 0, \tag{67}$$

$$D_1' r_\rho \ddot{r_\rho} + D_2' r_z \ddot{r_z} + \left(G_8 r_\rho^2 + G_9 r_z^2\right)\ddot{\alpha} + \left(G_{10} r_\rho^2 + G_{11} r_z^2\right)\dot{\alpha}^2 + \left(G_{12} r_\rho \dot{r_\rho} + G_{13} r_z \dot{r_z}\right)\dot{\alpha} + G_{14}\frac{\ell^2}{r_\rho^3} + \frac{4D_7'\gamma}{r_\rho^2 r_z} = 0, \tag{68}$$

whose initial conditions are given by the stationary equations (55)–(57). **In fig6 we have a comparison between vortex core size (r_ξ) and radial cloud size (r_ρ) while free expansion for three initial trap configurations. The fig6a agrees qualitatively with others numerical works [23, 32], since that vortex core size is defined for several ways when it has done numerically. Generally the vortex core expands faster than the condensate at early times, going to the same tax of expansion which can be noted an asymptotic behavior in all lines of fig6. It occurs due the vortex feeling an extra quantum pressure, both pressures submitted by radial and axial confinement, beyond its own kinetic energy. The prolate condensate ($\lambda = 0.1$, solid black line in fig6) has the ratio r_ξ/r_ρ almost constant, since the vortex is very long at z-direction it expands like radial component of the condensate. The isotropic condensate ($\lambda = 1$, dashed blue line in fig6) can be able to show us plainly the effects of its own kinetic contribution arising from quantized angular momentum. In oblate**

initial configuration ($\lambda = 10$, dotted red line in fig6), the vortex expands faster and faster other trap configuration ($\lambda < 10$) due high axial confinement. When $\ell > 1$ the vortex shows a superior kinetic energy, which can be seen comparing fig6b with fig6a. This result agrees qualitatively with our preview work [24], where the fig.6b could not be calculated since the authors considered the healing length as an approximation to the vortex core radius which is only valid for $\ell = 1$. This result exceeds [24] in at least 20%, being more accurate and general.

VII. CONCLUSIONS

In this paper we proposed a modification in the wave function phase commonly used with the variational method which corrects the imaginary frequencies of collective modes when we have a parameter describing non-physical vortex core dynamics with $\ell = 1$.

Here we consider variational phase parameters corresponding to each parameter in wave function amplitude, respectively. This way, we were able to describe the dynamics of both vortex core and the external dimensions of the condensate which agrees with the numerical simulations of the GPE. Although we observe four modes of oscillation in total, only three of them can be simultaneously observed depending on the trap anisotropy.

We also demonstrate that these oscillation modes can be excited by modulating the s-wave scattering length using the same experimental techniques as in Ref. [1].

Finally, we analyzed the time-of-flight dynamics of the vortex core with different circulations in order to complement the results in Ref. [24].

Acknowledgments

We acknowledge the financial support of from the National Council for the Improvement of Higher Education (CAPES) and from the State of São Paulo Foundation for Research Support (FAPESP).

[1] POLLACK, S. E. et al. Collective excitation of a bose-einstein condensate by modulation of the atomic scattering length. *Physical Review A*, v. 81, n. 5, p. 053627, 2010.

[2] STRINGARI, S. Collective excitation of a trapped bose-einstein-condensad gas. *Physical Review Letters*, v. 77, n. 12, p. 2360, September 1996.

[3] PÉREZ-GARCÍA, V. M. et al. Low energy excitations of a bose-einstein condensate: a time-dependent variational analysis. *Physical Review Letters*, v. 77, n. 27, p. 5320–5323, December 1996.

[4] DALFOVO, F. et al. Theory of bose-einstein condensate in trapped gases. *Reviews of Modern Physics*, v. 71, n. 3, p. 463–512, April 1999.

[5] COURTEILLE, P. W.; BAGNATO, V. S.; YUKALOV, V. I. Bose-einstein condensation of trapped atomic gases. *Laser Physics*, v. 11, n. 6, p. 659–800, 2001.

[6] BUSCH, T. et al. Stability and collective excitations of a two-component bose-einstein condensad gas: A moment approach. *Physical Review A*, v. 56, n. 4, p. 2978, October 1997.

[7] ZHANG, Z.; LIU, W. V. Finite-temperature damping of collective modes of a bcs-bec crossover superfluid. *Physical Review A*, v. 83, n. 2, p. 023617, 2011.

[8] HEISELBERG, H. Collective modes of trapped gases at the bec-bcs crossover. *Physical Review Letters*, v. 93, n. 4, p. 040402, July 2004.

[9] ALTMEYER, A. et al. Precision measurements of collective oscillations in the bec-bsc crossover. *Physical Review Letters*, v. 98, n. 4, p. 040401, January 2007.

[10] ČLOVEČKO, M. et al. New non-goldstone collective mode of bec of magnons in superfluid 3he-b. *Physical Review Letters*, v. 100, n. 15, p. 155301, April 2008.

[11] PETHICK, C. J.; SMITH, H. *Bose-einstein condensation in dilute gases*. 2nd. ed. Cambridge: Cambridge University Press, 2008.

[12] PITAEVSKII, L. P.; STRINGARI, S. *Bose-Einstein Condensation*. First edition. [S.l.]: Oxford University Press Inc, 2003.

[13] ZAMBELLI, F.; STRINGARI, S. Quantized vortices and collective oscilations of a trapped bose-einstein condensate. *Physical Review Letters*, v. 81, n. 9, p. 1754–1757, August 1998.

[14] BANERJEE, A.; TANATAR, B. Collective oscillations in a two-dimensional bose-einstein condensate with a quantized vortex state. *Physical Review A*, v. 72, p. 053620, November 2005.

[15] SVIDZINSKY, A. A.; FETTER, A. L. Dynamics of a vortex in a trapped bose-einstein condensate. *Physical Review A*, v. 62, p. 063617, November 2000.

[16] SVIDZINSKY, A. A.; FETTER, A. L. Stability of a vortex in a trapped bose-einstein condensate.

Physical Review Letters, v. 84, n. 26, p. 5919–5923, 2000.

[17] LINN, M.; FETTER, A. L. Small-amplitude normal modes of a vortex in a trapped bose-einstein condensate. *Physical Review A*, v. 61, p. 063603, May 2000.

[18] PÉREZ-GARCÍA, V. M.; GARCÍA-RIPOLL, J. J. Two-mode theory of vortex stability in multicomponent bose-einstein condensates. *Physical Review A*, v. 62, p. 033601, August 2000.

[19] KOENS, L.; MARTIN, A. M. Perturbative behavior of a vortex in a trapped bose-einstein condensate. *Physical Review A*, v. 86, p. 013605, July 2012.

[20] PÉREZ-GARCÍA, V. M. et al. Dynamics of bose-einstein condensates: variational solutions of the gross-pitaevskii equations. *Physical Review A*, v. 56, n. 2, p. 1424–1432, August 1997.

[21] SVIDZINSKY, A. A.; FETTER, A. L. Normal modes of a vortex in a trapped bose-einstein condensate. *Physical Review A*, v. 58, n. 4, p. 3168, October 1998.

[22] O'DELL, D. H. J.; EBERLEIN, C. Vortex in a trapped bose-einstein condensate with dipole-dipole interactions. *Physical Review A*, v. 75, n. 1, p. 013604, 2007.

[23] DALFOVO, F.; MODUGNO, M. Free expansion of bose-einstein condensates with quantized vortices. *Physical Review A*, v. 61, n. 2, p. 023605, January 2000.

[24] TELES, R. P. et al. Free expansion of bose-einstein condensates with a multicharged vortex. *Physical Review A*, v. 87, n. 3, p. 033622, March 2013.

[25] HENN, E. A. de L. *Produção experimental de excitações topológicas em um condensado de Bose-Einstein. 2008. 129p.* Tese (Doutorado) — Instituto de Física de São Carlos, Universidade de São Paulo, São Carlos, 2008.

[26] DENNIS, G. R.; HOPE, J. J.; JOHNSSON, M. T. Xmds2: Fast, scalable simulation of coupled stochastic partial differential equations. *Computer Physics Communications*, v. 184, n. 1, p. 201–208, January 2013.

[27] KETTERLE, W. The magic of matter waves. *MIT Physics Annual*, p. 44–49, 2001.

[28] HENN, E. A. L. et al. Observation of vortex formation in an oscillating trapped bose-einstein condensate. *Physical Review A*, v. 79, n. 4, p. 043618, 2009.

[29] HENN, E. A. L. et al. Emergence of turbulence in an oscillating bose-einstein condensate. *Physical Review Letters*, v. 103, n. 4, p. 045301, July 2009.

[30] CHEVY, F.; MADISON, K. W.; DALIBARD, J. Measurement of the angular momentum of a rotating bose-einstein condensate. *Physical Review Letters*, v. 85, p. 2223–2227, 2002.

[31] ANDERSON, B. P.; HALJAN, P. C. Vortex precession in bose-einstein condensates: observartions with filled and empty cores. *Physical Review Letters*, v. 85, n. 14, p. 2857–2860, October 2000.

[32] LUNDH, E.; PETHICK, C. J.; SMITH, H. Vortices in bose-einstein-condensed atomic clouds. *Physical Review A*, v. 58, n. 6, p. 4816–4823, December 1998.